

Mechanics of the plowing experiment of the poroelastic and hyperelastic biomaterial

MKP model poroelastického a hyperelastického materiálu zatíženého pohybujícím se indentorem

Ing. Michala Čadová

Vedoucí práce: RNDr. Matej Daniel Ph.D.

Abstrakt

Znalost mechanických vlastností biologických materiálů je klíčová v oblastech, jako je tkáňové inženýrství, návrh implantátů a predikce poškození biomateriálů vlivem vnějšího zatížení. Během většiny zkoušek biologických materiálů je vzorek zatěžován pouze v jednom směru, zatímco v případě reálné biologické tkáně se jedná o kombinované namáhání. Proto byl na Klinice pro poruchy žvýkacího systému na Univerzitě v Curychu (Švýcarsko) vyvinut „Rolling Plowing Explants Test System“ (RPETS), který zatěžuje vzorek ve dvou směrech. Protože se časové a prostorové rozložení některých biomechanických veličin nedá experimentálně změřit, využívá se k tomuto účelu matematických modelů, které jsou v dnešní době založeny převážně na metodě konečných prvků.

Cílem této práce bylo vyšetřit mechanickou odezvu vzorků z poroelastického a hyperelastického materiálu při zatěžování na RPETS. Vzorky měly idealizovanou geometrii a měření a model byli provedeny pouze dvourozměrně. Validace modelu je založena na porovnání hodnot posunutí a síly indentoru získaného z matematického modelu s hodnotami z experimentu během jednoho zatěžovacího cyklu.

Klíčová slova

Plowing, poroelastický materiál, hyperelastický materiál, temporomandibulární kloub, kloubní chrupavka, metoda konečných prvků

1. Introduction

Disorders of TMJ affect 3-29 % people (Spilker *et al.* 2009) (while the slight indications of degenerative disease in TMJ can be found between 25 and 35 years (Pullinger *et al.* 1988). TMJ consists of fossa of the maxilla, a condyle of the mandible and a cartilaginous disc. Especially the cartilaginous disc undergoes large deformation and displacement. Its function is to reduce frictional forces between fossa and condyle. It acts a stress absorber, as well (Tanaka *et al.* 2003). The TMJ disc can adapt its shape accordingly to the shape of articulating surfaces. By distributing the force over a larger contact area the peak values of the stress field are reduced (Detamore *et al.* 2003a, Tanaka *et al.* 2006). To prevent the degenerative changes and other disorders of the TMJ and disc, we need to understand properly the mechanical and biochemical structure of these tissues as well as the loading conditions in the joint and between its individual parts.

The TMJ disc is basically a cartilaginous tissue; therefore general description of cartilaginous material can be applied to the disc, as well. Cartilage, especially articular cartilage, is a biological material, which surface is smooth and glistening. This facilitates a smooth motion within the joint. Since cartilage is an aneural tissue, i.e. without blood

supply, nutrition is gain by diffusion from the synovial fluid in the joint capsule. From 70 to 85 % of its weight is made of interstitial fluid. The hard part of the tissue is composed from cells and multicomponent matrix. Dominant part of the matrix comprises from proteoglycans and collagen. Further and detailed description of the articular cartilage and its mechanical and biochemical composition can be found in the literature (Tanaka *et al.* 2003, Ateshian *et al.* 1997, Bullough *et al.* 1968, Levangie *et al.* 2005, Levangie *et al.* 2005, Mansour 2004, Mansour 2004, Wilson *et al.* 2005, Mow *et al.* 1980, Mow *et al.* 2002, Clarke 1971, Davies *et al.* 1962, Policard 1936). Furthermore, the TMJ disc has some unique properties that facilitate its formidable function. It has a flexible central part, its properties depends on the direction and type of the loading, it become stiffer as the loading rate increases, etc. (Tanaka *et al.* 2003, Detamore *et al.* 2003a, Detamore *et al.* 2003b, Chin *et al.* 1996, Kuo *et al.* 2010, Piette 1993, Tanaka *et al.* 1999, Tanaka *et al.* 2000, Tanaka *et al.* 2008).

Mechanical properties of articular cartilage are tightly connected to its biochemical composition and structure. The most significant property of the cartilage is the viscoelasticity. That means that the tissue behaviour is dependent no only on the external loading conditions history but also the time. Generally, after cease of the external load viscoelastic materials are capable of gain their initial condition. These materials are sensitive to the rate of loading, and exhibits time-dependent creep and stress-relaxation (Tanaka *et al.* 2003, Mow *et al.* 2002, Tanaka *et al.* 1999).

Loading patterns in TMJ are very specific. Plowing forces are produced by the deformation of the cartilage matrix as a stress-field translates over the surface (Coles *et al.* 2008, Gallo *et al.* 2000, Mow *et al.* 1993, Nickel *et al.* 2004, Nickel *et al.* 2006, Nickel *et al.* 2009). Frictional force occurs “due to rubbing of the cartilage surfaces” (Gallo *et al.* 2000, Nickel *et al.* 2004). These two types of forces results in tractional forces (Spilker *et al.* 2009, Nickel *et al.* 2004). Tractional forces associated with static and dynamic friction on the surface of the TMJ disc are low (Nickel *et al.* 2004, Nickel *et al.* 2001, Nickel *et al.* 2001). On the other hand, experimental results indicate that the plowing forces on the surface are much higher (at least an order of magnitude greater) than the friction forces (Spilker *et al.* 2009, Nickel *et al.* 2004, Nickel *et al.* 2006, Nickel *et al.* 2009).

It is difficult to measure the plowing forces *in vivo*. Therefore, the *in vitro* experimental methods for plowing forces evaluation are used (Spilker *et al.* 2009). From these kinds of experiments, not only the relationship between the applied load and the resultant mechanical changes of the tissue can be determined. The biological and biochemical changes of the tissue under the prescribed load can make part of the results, as well. However, the plowing experiment alone cannot give us a whole image of the relationship between loading, and mechanical, and biochemical response of the tissue. Besides an experiment *in vivo/in vitro*, a computational method should be used to create a validated model that could be used for further exploration of spatial and time distribution of biomechanical variables within the tissue (Spilker *et al.* 2009). A computer simulation using the finite element analysis (FEM, ABAQUS, Inc., Providence, RI, USA) and biphasic/poroelastic mathematical model (Mow *et al.* 1980, Ateshian *et al.* 1994, Ateshian *et al.* 1995, Mow *et al.* 1984, Wu *et al.* 1998a) proved to be a useful tool for modelling biomechanical processes (Donzelli *et al.* 2004, Goldsmith *et al.* 1996, Spilker *et al.* 1992, Tanaka *et al.* 1994, Wayne *et al.* 1991, Wu *et al.* 1998b).

At the Clinic for Masticatory Disorders at the University of Zurich, Switzerland, a loading device, that can simulate the TMJ disc loading *in vitro*, was developed (Rolling Plowing Explants Test System (RPETS, Colombo *et al.* 2011). In contrast with most testing devices, and even some bioreactors, that load the (biological) sample only in one direction, this device can integrate more than one type of force to better reflect the physiological forces that biomaterial experience *in vivo*.

The objective of this study was to estimate mechanical behaviour of idealized two-dimensional samples with different material properties (poroelastic and hyperelastic materials) that are under a complex loading in the RPETS. Approximate validation of the plowing model was based on comparison of model-predicted displacements and vertical forces of the indenter to experimental measurements during one cycle of the plowing motion.

Prospective plans are to determine a relationship between the mechanical response of the biomaterial, gained from the model, and biochemical response acquired from the experiment.

2. Materials and methods

2.1 In vitro plowing experiment

In the Laboratory of Physiology and Biomechanics of the Masticatory System (University of Zurich, Switzerland) were in recent years several plowing experiments of cartilage conducted. As tissue model, a bovine nasal septum (BNS) was used. This tissue proved to have highly viscoelastic behavior, i.e. material properties comparable with the TMJ disc, yields well reproducible results in terms of geometry, mechanical properties and cell viability; and is largely available. During the experiment, pure plowing (Figure 1) was applied on the cartilaginous strip (Figure 2).



Figure 1. Plowing experiment settings. Cartilaginous strip (2x20x60 mm) was glued to the bottom of the basin, which was filled with physiological solution that was kept at constant temperature 37°C. The steel indenter (\varnothing 25 mm, high 40 mm) was lowered to the sample (force of 25 N, 50 N or 100 N was kept constant) and moved in the longitudinal axis of the sample with velocity of trapezoidal profile (10 mm/s peak value). Cyclic loading lasted 2 hours.

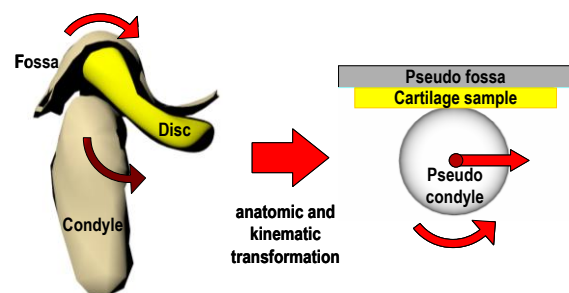


Figure 2. Idealization of the TMJ disc.

A strip of approximate dimension 2x20x60 mm was used. It was glued to the bottom of a basin either with the whole bottom surface or only by the end parts of the bottom surface (Figure 5). The basin, in which the sample was submerged, was filled with physiological solution (to mimic the in vivo environment and to keep the cells alive) whose temperature was kept constant (37 °C). A steel indenter (\varnothing 25 mm) was lowered into the strip and then moved with the prescribed velocity (trapezoidal profile, 10 mm/s peak value) along the longitudinal axis of the sample. The applied force was kept constant at 25 N, 50 N or 100 N. These settings were intended to simulate the motion of the condyle on the TMJ disc (Figure 2). Cyclic loading lasts for 2 hours which corresponds to approximately 480 cycles. The

parameters of the plowing experiment were based on data, that were acquired *in vivo* by means of dynamic stereometry (Gallo 2005, Palla *et al.* 2003).

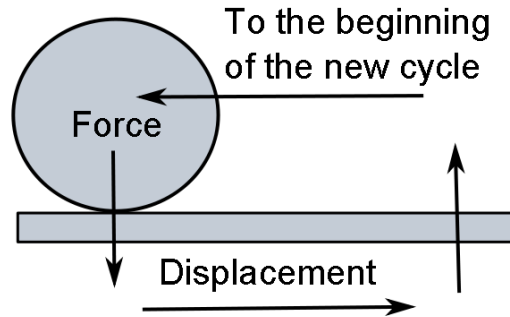


Figure 3. Schematic representation of the plowing test. Firstly, the sample is compressed via a steel indenter. Next, the indenter moves along the longitudinal direction of the sample with prescribed displacement. In the end of the sample, the indenter is unloaded and returns to its initial position.

The experiment using the BNS was primarily set up to evaluate the biological response of bovine cartilage explants to mechanical loading mimicking the plowing loading as measured *in vivo*. It was proved that two hours duration is reasonable for the biological changes in the tissue to occur. Nevertheless, for the pure mechanical investigation, only one loading cycle was of my interest. The sampling frequency of data acquisition was 1 Hz.

In addition to the poroelastic material, a hyperelastic material, which was already used for the RPETS validation (Colombo *et al.* 2011), was used, as well. Advantage of this non-biological material is a good reproducibility of the measured values and easier test procedures since no special care must be implied as with the biomaterials. The sampling frequency of data acquisition was 1 kHz.

Vertical and horizontal (tractional) forces were measured using a platform load cell and button load cell, respectively. The displacement of the probe was measured using a linear variable differential transformer (LVDT).

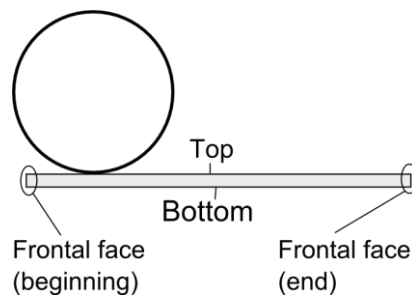


Figure 4. Faces definition related to the model and sample description.

2.2 Material and sample geometry definition

For the BNS sample a user incisory texture was used, therefore, all the samples has a constant geometry of 2x2x60 mm. Mechanical properties of BNS were taken from the previous experiments conducted at the Laboratory of Physiology and Biomechanics of the Masticatory System (University of Zurich, Switzerland). Static stress-relaxation tests in confined and unconfined compression were performed. Results from the equilibrium response gave average values for aggregate modulus $H_A = 2.15 \pm 0.5 \text{ MPa}$, Young modulus $E = 1.98 \pm 0.6 \text{ MPa}$ and the Poisson ratio $\nu = 0.22 \pm 0.07$. For the first approach a constant permeability of $k = 3.22 \pm 0.5 \times 10^{-15} \text{ m}^4 / (\text{Ns})$ was used.

Mechanical behaviour of the hyperelastic material was determined in a uniaxial tensile test performed with MTS Mini Bionix testing machine (MTS, Eden Prairie, USA) in the Laboratory of Biomechanics of the Faculty of Mechanical Engineering of the Czech Technical University in Prague (Prague, Czech Republic). The sample of latex strip has been recording by CCD camera during the extension. The photographs of the strip were evaluated with Matlab (MathWork Inc., USA) utility Imconture 7 which employs Canny algorithm for the edge detection in a digital image. The edge detection gave us information about extension of the sample. Loading force was measured by MTS testing machine. The material definition was than based on the stress-strain curve acquired from the experimental measurement.

2.3 Finite element simulation of the plowing experiment

The cartilaginous strip as well as the strip of the hyperelastic material, is modeled using an idealized geometry. Only a two-dimensional (2D) (Figure 2 and Figure 3) representation of the samples was performed. There are several reasons for this approach. Firstly, results, such as the indenter force and displacement, from the real plowing experiment were collected only in one plane. Therefore, any data were at our disposal for the validation of the model in the third dimension. Secondly, we have assumed that the indenter's major impact will be in the direction of its forward displacement, i.e. only in one plane. Finally, a 2D model is much less computationally demanding than the 3D model.

Cartilaginous tissue - A biphasic material representation (Mow *et al.* 1980) was chosen for the cartilaginous tissue representation. This material model has proven its ability to describe well the solid-fluid coupling in the porous material, such as cartilage (Donzelli *et al.* 2004). In the existing model no cartilage layers were taken into account and the sample was model as a homogenous material.

Depending on the type of gluing of the sample to the bottom of the basin (Figure 5), different boundary conditions were applied in the model. However, for all the three cases the same free-draining surface conditions (i.e. interstitial fluid can freely flow out) were applied to the top and both frontal faces of the sample (Figure 4). The mesh density of the sample was set as 20x300 and the quad structured CPE4P elements were used.

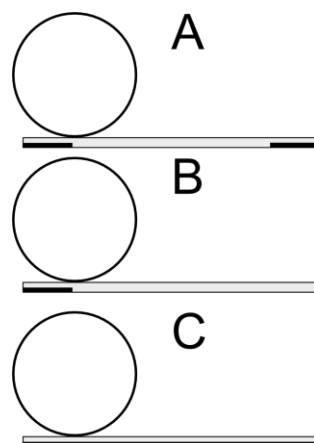


Figure 5. Different type of gluing of the sample: A) with both end-bottom area, B) with only one end-bottom area that is near the edge where the indenter's movement begins, C) with the whole bottom surface.

Hyperelastic material - The geometry of this sample and the loading conditions are the same as for the poroelastic model. Because of greater deformation a denser mesh and gluing of the whole bottom were applied to avoid huge bulging of the unattached material (Figure 6).

The hyperelastic material model in Abaqus is isotropic and nonlinear. It is valid for materials that exhibit instantaneous elastic response up to large strains. In Abaqus,

hyperelastic materials are described in terms of a “strain energy potential”, which defines the strain energy stored in the material per unit of the volume in the initial configuration as a function of the strain at that point in the material. There are several forms of strain energy potentials available in Abaqus to model approximately incompressible isotropic elastomers. The Marlow form together with the data from the stress-strain curve was used. The quad, structured, linear, plane stress elements were used (CPS4).

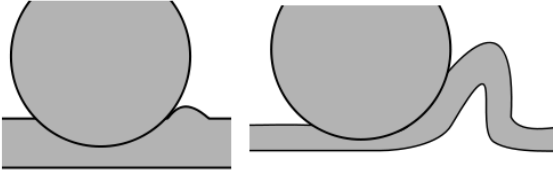


Figure 6. Example of bulging for two different type of the sample attachment. Left: whole bottom of the sample is glued to the bottom of the basin and bulging occurs only in the upper area of the sample. Right: sample is glued to the bottom of the basin with only both end-bottom areas and bulging occurs through the whole thickness of the sample.

3. Results

Vertical and horizontal forces and displacements of the indenter were measured during the experiment and subsequently compared with the values gained from the FE model.

3.1 Hyperelastic model

Since the hyperelastic material can undergo large deformation under the external load, the whole bottom of the sample was glued to the bottom of the basin (Figure 5 C) to avoid the vertical bulging of the unattached part of the sample (Figure 6 right). Three different loading magnitudes were applied: 25 N, 50 N, and 100 N.

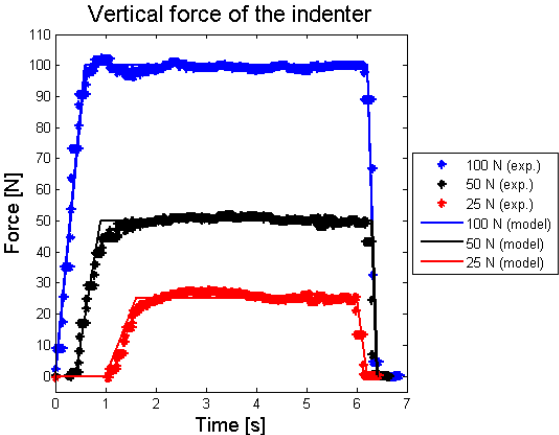


Figure 7. Vertical reaction force of the indenter measured during the loading phase of one cycle of the experiment. The FE model prediction of the vertical force coincides with the prescribed loading curve of the indenter.

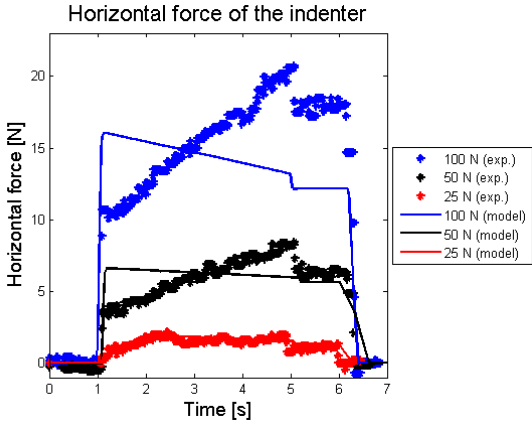


Figure 8. Horizontal reaction force of the indenter gained from the experimental measurement and the FE simulation.

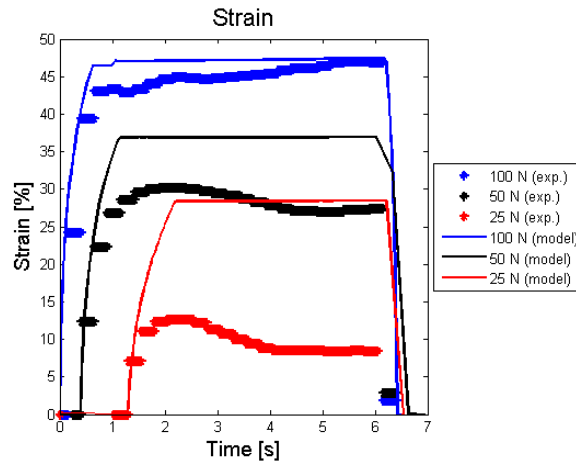


Figure 9. Strain of the cartilaginous sample computed from the initial idealized thickness of the sample and vertical displacement of the indenter measured during one loading cycle. For the FE model, the logarithmic strain was taken directly from the FEM model results.

Table 1 Maximal stress and strain in the poroelastic material for three different applied loads in the vertical direction.

Vertical force of the indenter	25 N	50 N	100 N
Max. stress (in compression) [MPa]	0,216	0,366	0,586
Max. compressive strain [-]	0,353	0,516	0,757

3.2 Poroelastic model

Not only three different applied vertical forces, but also three different types of gluing of the sample (Figure 5) were applied. First of all, data acquired from the experiment were compared with the same set of data gained from the finite element model. The horizontal and vertical force and displacement of the indenter were measured.

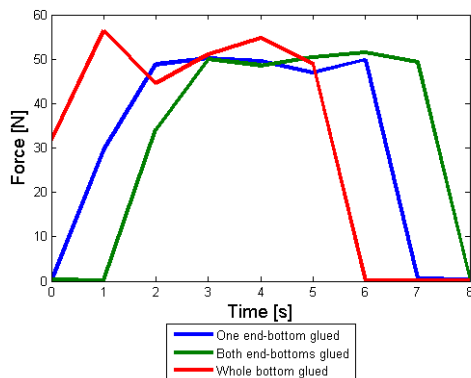


Figure 10. Data from the experiment for the reaction force of the indenter in the vertical direction for three different types of sample attachment. Prescribed vertical force of the indenter was 50 N.

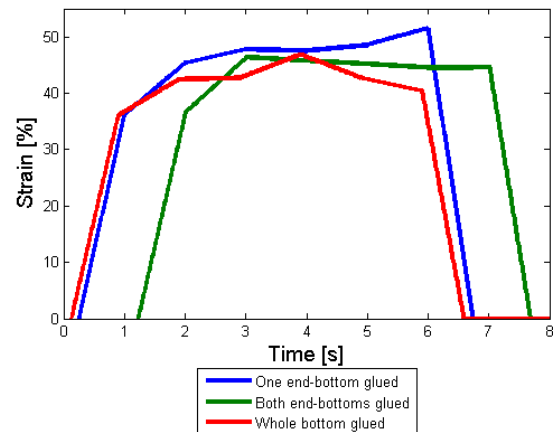


Figure 11. Data from the experiment for the sample strain. Values for three different types of sample attachment are depicted. Vertical force of the indenter was 50 N.

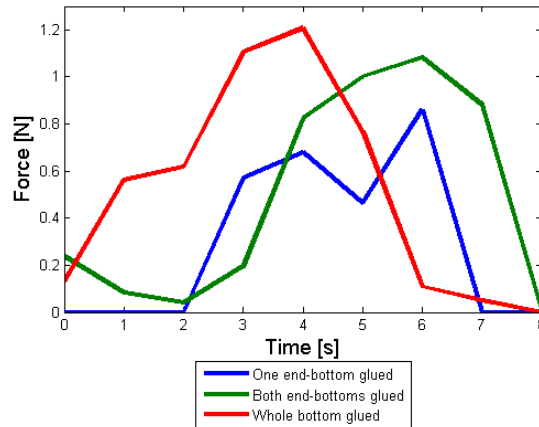


Figure 12. Data from the experiment for the reaction force of the indenter in the horizontal direction for three different types of sample attachment. Vertical force of the indenter was 50 N.

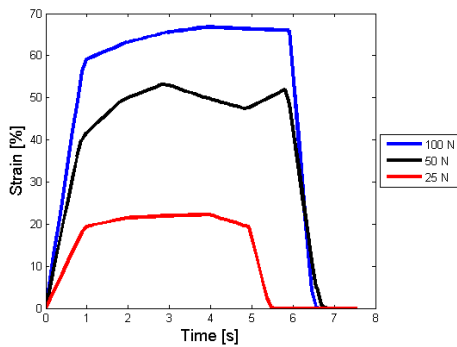


Figure 13. Strain of the cartilaginous tissue under three different vertical loads of the indenter (experimental data; sample is glued to the basin with both end-bottom areas).

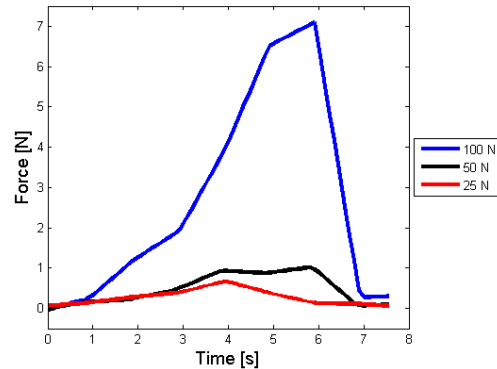


Figure 14. Horizontal reaction force of the indenter. Comparison for three different vertical loads (experimental data; sample is glued to the basin with both end-bottom areas).

Unlike the results from the experimental measurement, the FE model predict smaller strain (smaller indenter's vertical displacement), but higher horizontal force. The vertical force and the horizontal displacement of the indenter match the prescribed function and the experimental results.

Table 2 Comparison of the maximal strain and maximal stress of the cartilaginous sample for three different applied loads.

Vertical force of the indenter	25 N	50 N	100 N
Max. horizontal force of the indenter [N]	10	15	20
Max. compressive strain [%]	12,5	18,5	35

4. Discussion

4.1 Hyperelastic material

Sampling frequency of data acquisition for the hyperelastic sample was 1 kHz. From the resultant curve that depicts the vertical and horizontal force (Figure 7 and Figure 8) and

displacement, one can state, that for such a material sampling frequency of 100 Hz or even smaller (10 Hz) would be satisfying.

Comparing the experimental results and the results from the FE model, we can conclude, that with increasing force that is applied to the indenter in the vertical direction, the maximal depth of indentation increases from 0,25 mm for the 25 N to 0,7 mm for 100 N (Figure 9). The depth of indentation (change in the sample thickness) was converted to logarithmic strain, so that these results can be compared with the results from the FE model. Initial thickness of the sample was assumed constant with value of 2 mm. Depth of indentation predicted by the FE model is higher than the experimental results (Figure 9). Moreover, results from the FE simulation from the middle of the loading cycle (the cruise phase) stay at a constant value, whereas experimental values show increasing (for the vertical load of 100 N) or decreasing (for vertical load of 25 N and 50 N) tendency. This can be caused by an idealized geometry of the FE model. Figure 9 also shows that with increasing applied force in the vertical direction, model matches the experimental result better.

What the model predicts poorly is the reaction force of the indenter in the horizontal direction. Experimental results show increasing force throughout the loading cycle whereas model predicts decreasing horizontal force (Figure 8). That means, that in the model, the maximal horizontal force of the indenter is reached in the beginning of the cycle, whereas in the experiment in the end. Both results seem reasonable. The maximal vertical force in the end is caused by bulging (Figure 6) of the unattached material which is pushed in front of the front face of the indenter and therefore, with increasing time, the amount of such bulging slightly increases and causes higher horizontal force. On the other hand, high force in the beginning of loading can be influence by the difference in the static and kinetic coefficients of friction. Figure 8 shows that with the FE model match the experimental result better with decreasing force. Table 1 contains numerical values of maximal stress and strain in the sample for the three vertical loading forces.

4.2 Poroelastic material

Three type of sample attachment were experimentally measured only for the vertical loading force of 50 N. On the other hand, for the case when the sample was glued with both end-bottom areas (Figure 5 A), three different vertical forces were applied. Then, influence of different loading on the mechanical changes for this type of attachment was compared.

Type of the gluing has a little influence on depth of the indentation (Figure 11) and the vertical reaction force (Figure 10). However, the horizontal reaction force of the indenter is influenced considerably (Figure 12). From this result we can state, that the smallest tractional (horizontal) force appears for the case with only one end-bottom area glued, whereas the largest force occurs for the case with the whole bottom glued. This is cause mainly by bulging of the material (Figure 6 right).

Since the experiment using the BNS was primarily set up to evaluate the biological response of bovine cartilage explants to mechanical loading, death of cells, which were in contact with the gluing substance, was in our interest as well. That is why the case with the smallest glued area, but high strength of the contact was chosen (Figure 5 A). This type of attachment ensures satisfying stability of the sample in the tank and cause death of only small number of cells. On the other hand, only in this case, the huge bulging occurs. That means, that the material along the whole thickness is deformed and free (to some extent) to move in the vertical direction. However, this type of movement is not really physiological. If we still think about this type of plowing experiment as a representation of the loading of the TMJ disc, we should for the oncoming experiment re-evaluate the type of sample attachment, even though it will have an unfavorable impact on the number of living cells at the end of the experiment.

From the experimental measurement and data processing strain in the sample range from approximately 20 % for the 25 N vertical loads to 68 % for vertical force of 100 N (Figure 13). These values are considerably higher than the strain gain from the FE model. The FE model predict strain values of the cartilaginous sample from 12,5 % for 25 N force to 35 % for 100 N force (Table 2), which seems more reasonable. Different methodology of measuring the vertical displacement of the indenter and consequently the change of the sample thickness should be applied. From the current settings, the vertical force and displacement of the indenter is measured and from these values the change in thickness of the sample is indirectly determined.

In contrast to the strain which reaches high values in the real experiment, the horizontal force reaches higher values in the FE simulation (Figure 14, Table 2). Even though, the “sample-indenter” contact was assumed as frictionless, the difference in the horizontal force is nearly three fold.

Even though, the FE model did not prove the ability to properly describe the real plowing experiment, some of other mechanical variables were investigated. From comparison of the normal stress and the fluid pressure gained from the FE model, we can read that the fluid takes up at least 60 % of the load. In the literature it is in most cases reported that the fluid phase carries more than 90 % of the load (Spilker *et al.* 2009). Therefore, these results of our model should be further investigated. Nevertheless, load bore by the fluid phase depends on the permeability of the fluid, the void ratio between the fluid and solid phase of the whole tissue and other variables, which are not the same not only between the species, but also within one organism. Therefore, interpretation of the results must be done carefully.

There are several ways how to improve the experimental and FE model results agreement. Firstly, the methodology of strain computation during the experiment should be re-evaluated. Secondly, material properties of the cartilaginous sample should be checked. Next, the different FE material model can be considered (anisotropic instead of isotropic). Finally, boundary condition and model attachment should be revised.

5. Conclusion

Hyperelastic material - The hyperelastic model matches the experimental data only to some extent. Improvement of the model is needed. The improvement can be done either by change of material model definition or by different combination of FE mesh and element types.

Poroelastic material - Even though, some discrepancies between the model and reality exist, the poroelastic model proves a good ability to describe the behaviour of the sample during the experimental conditions. The distribution of stress, strain, pore pressure and fluid flow were investigated.

From existing analysis, FE simulations, and data acquisition, several conclusions were made to 1) improve oncoming experiments and methods to gain data from these tests, 2) improve the model so that it describes the real behaviour of the cartilaginous tissue more precisely.

Acknowledgments

This work was supported by the Grant Agency of the Czech Technical University in Prague, grant No. SGS10/247/OHK2/3T/12 and by Sciex-NMS^{ch}. I would like to thank Matej Daniel and Luigi M. Gallo for their help with the cartilage mechanobiology part of this work, Rita Corroero for her results from the RPETS experiment and Zdenek Horak for his help concerning the FEM software ABAQUS.

Literature

- ATESHIAN, G. A., et al. An Asymptotic Solution for the Contact of Two Biphasic Cartilage Layers. *Journal of Biomechanics*. 1994, vol. 27, no. 11, s. 1347-1360.
- ATESHIAN, G. A.; WANG, H. A Theoretical Solution for the Frictionless Rolling Contact of Cylindrical Biphasic Articular Cartilage Layers. *Journal of Biomechanics*. 1995, vol. 28, no. 11, s. 1341-1355.
- ATESHIAN, G. A., et al. Finite Deformation Biphasic Material Properties of Bovine Articular Cartilage from Confined Compression Experiments. *Journal of Biomechanics*. 1997, vol. 30, no. 11-12, s. 1157-1164.
- BULLOUGH, P.; GOODFELLOW, J. The Significance of the Fine Structure of Articular Cartilage. *The Journal of Bone and Joint Surgery, British Volume*. 1968, vol. 50, no. 4, s. 852-857.
- CHIN, L. P.; AKER, F. D.; ZARRINIA, K. The Viscoelastic Properties of the Human Temporomandibular Joint Disc. *Journal of Oral and Maxillofacial Surgery: Official Journal of the American Association of Oral and Maxillofacial Surgeons*. 1996, vol. 54, no. 3, s. 315-8; discussion 318-9.
- CLARKE, Ian C. Articular Cartilage: A Review and Scanning Electron Microscope Study. *Journal of Bone and Joint Surgery - British Volume*. 1971, vol. 53, no. 4, s. 732-750.
- COLES, J.M., et al. In Situ Friction Measurement on Murine Cartilage by Atomic Force Microscopy. *Journal of Biomechanics*. 2008, vol. 41, no. 3, s. 541-548.
- COLOMBO, V., et al. (*in press*) Design, Construction and Validation of a Computer Controlled System for Functional Loading of Soft Tissue. *Medical Engineering & Physics*.
- DAVIES, D. V., et al. Electron Microscopy of Articular Cartilage in the Young Adult Rabbit. *Annals of the Rheumatic Diseases*. 1962, vol. 21, no. 11.
- DETAMORE, M.S.; ATHANASIOU, K.A. Motivation, Characterization, and Strategy for Tissue Engineering the Temporomandibular Joint Disc. *Tissue Engineering*. 2003a, vol. 9, no. 6, s. 1065-1087.
- DETAMORE, M.S.; ATHANASIOU, K.A. Tensile Properties of the Porcine Temporomandibular Joint Disc. *Journal of Biomechanical Engineering*. 2003b, vol. 125, no. 4, s. 558-565. ISSN 0148-0731; 0148-0731.
- DONZELLI, P. S., et al. Biphasic Finite Element Simulation of the TMJ Disc from in Vivo Kinematic and Geometric Measurements. *Journal of Biomechanics*. 2004, vol. 37, no. 11, s. 1787-1791.
- GALLO, L. M., et al. Stress-Field Translation in the Healthy Human Temporomandibular Joint. *Journal of Dental Research*. 2000, vol. 79, no. 10, s. 1740-1746.
- GALLO, L. M. Modeling of Temporomandibular Joint Function using MRI and Jaw-Tracking Technologies--Mechanics. *Cells, Tissues, Organs*. 2005, vol. 180, no. 1, s. 54-68.
- GOLDSMITH, A. A. J.; HAYES, A.; CLIFT, S. E. Application of Finite Elements to the Stress Analysis of Articular Cartilage. *Medical Engineering & Physics*. 1996, vol. 18, no. 2, s. 89-98.
- KUO, Jonathan, et al. The Region-Dependent Biphasic Viscoelastic Properties of Human Temporomandibular Joint Discs Under Confined Compression. *Journal of Biomechanics*. 2010, vol. 43, no. 7, s. 1316-1321.
- LEVANGIE, Pamela K.; NORKIN, Cynthia C. *Joint Structure and Function: A Comprehensive Analysis*. fourth. ed. Philadelphia : F.A.Davis Company, 2005. 588 s.

- MANSOUR, J. M. *Kinesiology: the mechanics and pathomechanics of human movement*. . A. O. CAROL. Lippincott Williams & Wilkins. 2004. Biomechanics of Cartilage. s. 66-79. ISBN 0781774225.
- MOW, V. C.; ATESHIAN, G. A.; SPILKER, R. L. Biomechanics of Diarthrodial Joints: A Review of Twenty Years of Progress. *Journal of Biomechanical Engineering*. 1993, vol. 115, no. 4B, s. 460-467.
- MOW, V. C.; GUO, X. E. Mechano-Electrochemical Properties of Articular Cartilage: Their Inhomogeneities and Anisotropies. *Annual Review of Biomedical Engineering*. 2002, vol. 4, s. 175-209.
- MOW, V. C.; HOLMES, M. H.; LAI, W. M. Fluid Transport and Mechanical Properties of Articular Cartilage: A Review. *Journal of Biomechanics*. 1984, vol. 17, no. 5, s. 377-394.
- MOW, V. C., et al. Biphasic Creep and Stress Relaxation of Articular Cartilage in Compression: Theory and Experiments. *Journal of Biomechanical Engineering*. 1980, vol. 102, no. 1, s. 73-84.
- NICKEL, J. C., et al. Laboratory Stresses and Tractional Forces on the TMJ Disc Surface. *Journal of Dental Research*. 2004, vol. 83, no. 8, s. 650-654.
- NICKEL, J. C., et al. Static and Dynamic Loading Effects on Temporomandibular Joint Disc Tractional Forces. *Journal of Dental Research*. 2006, vol. 85, no. 9, s. 809-813.
- NICKEL, J. C., et al. The Effect of Disc Thickness and Trauma on Disc Surface Friction in the Porcine Temporomandibular Joint. *Archives of Oral Biology*. 2001, vol. 46, s. 155-162.
- NICKEL, J. C., et al. Static and Dynamic Mechanics of the Temporomandibular Joint: Plowing Forces, Joint Load and Tissue Stress. *Orthodontics & Craniofacial Research*. 2009, vol. 12, no. 3, s. 159-167.
- PALLA, S.; GALLO, L. M.; GOSSI, D. Dynamic Stereometry of the Temporomandibular Joint. *Orthodontics & Craniofacial Research*. 2003, vol. 6 Suppl 1, s. 37-47.
- PIETTE, E. Anatomy of the Human Temporomandibular Joint. an Updated Comprehensive Review. *Acta Stomatologica Belgica*. 1993, vol. 90, no. 2, s. 103-127.
- POLICARD, A. *Physiologie générale des articulations a l'éta normal et pathologique*. Paris: Masson et Cie, 1936s.
- PULLINGER, A. G.; SELIGMAN, D. A.; SOLBERG, W. K. Temporomandibular Disorders. Part I: Functional Status, Dentomorphologic Features, and Sex Differences in a Nonpatient Population. *The Journal of Prosthetic Dentistry*. 1988, vol. 59, no. 2, s. 228-235.
- SPILKER, R. L.; NICKEL, J. C.; IWASAKI, L. R. A Biphasic Finite Element Model of in Vitro Plowing Tests of the Temporomandibular Joint Disc. *Annals of Biomedical Engineering*. 2009, vol. 37, no. 6, s. 1152-1164.
- SPILKER, R. L.; SUH, J. K.; MOW, V. C. A Finite-Element Analysis of the Indentation Stress-Relaxation Response of Linear Biphasic Articular-Cartilage. *Journal of Biomechanical Engineering-Transactions of the Asme*. 1992, vol. 114, no. 2, s. 191-201.
- TANAKA, E.; KOOLSTRA, J. H. Biomechanics of Temporomandibular Joint. *Journal of Dental Research*. 2008, vol. 87, no. 11, s. 989-991.
- TANAKA, E., et al. Viscoelastic Properties of the Human Temporomandibular Joint Disc in Patients with Internal Derangement. *Journal of Oral and Maxillofacial Surgery : Official Journal of the American Association of Oral and Maxillofacial Surgeons*. 2000, vol. 58, no. 9, s. 997-1002.
- TANAKA, E., et al. Viscoelastic Properties of Canine Temporomandibular Joint Disc in Compressive Load-Relaxation. *Archives of Oral Biology*. 1999, vol. 44, no. 12, s. 1021-1026.

- TANAKA, E.; TANNE, K.; SAKUDA, M. A Three-Dimensional Finite Element Model of the Mandible Including the TMJ and its Application to Stress Analysis in the TMJ during Clenching. *Medical Engineering & Physics*. 1994, vol. 16, no. 4, s. 316-322.
- TANAKA, E.; VAN EIJDEN, T. Biomechanical Behavior of the Temporomandibular Joint Disc. *Critical Reviews in Oral Biology & Medicine*. 2003, vol. 14, no. 2, s. 138-150.
- TANAKA, E., et al. Dynamic Compressive Properties of the Mandibular Condylar Cartilage. *Journal of Dental Research*. 2006, vol. 85, no. 6, s. 571-575.
- WAYNE, J. S.; WOO, S. L.; KWAN, M. K. Application of the u-p Finite Element Method to the Study of Articular Cartilage. *Journal of Biomechanical Engineering*. 1991, vol. 113, no. 4, s. 397-403.
- WILSON, W., et al. The Role of Computational Models in the Search for the Mechanical Behaviour and Damage Mechanisms of Articular Cartilage. *Medical Engineering & Physics*. 2005, vol. 27, s. 810-826.
- WU, J. Z.; HERZOG, W.; EPSTEIN, M. Articular Joint Mechanics with Biphasic Cartilage Layers Under Dynamic Loading. *Journal of Biomechanical Engineering*. 1998a, vol. 120, no. 1, s. 77.
- WU, J. Z.; HERZOG, W.; EPSTEIN, M. Evaluation of the Finite Element Software ABAQUS for Biomechanical Modelling of Biphasic Tissues. *Journal of Biomechanics*. 1998b, vol. 31, no. 2, s. 165-169.